RSC Advances

PAPER

View Article Online
View Journal | View Issue

Cite this: *RSC Adv.*, 2016, **6**, 25975

Hydrogen production from biomass by continuous fast pyrolysis and in-line steam reforming

A. Arregi, G. Lopez, M. Amutio,* I. Barbarias, J. Bilbao and M. Olazar

The continuous fast pyrolysis (500 °C) of pine wood sawdust has been studied in a conical spouted bed reactor (CSBR) followed by in-line steam reforming of the pyrolysis vapours in a fluidised bed reactor on a Ni commercial catalyst. An analysis has been carried out on the effect reforming temperature in the 550–700 °C range, space time from 2.5 to 30 g_{cat} min $g_{volatiles}^{-1}$ and steam/biomass ratio between 2 and 5 have on the pyrolysis volatile conversion, H_2 yield and gaseous stream composition. The continuous pyrolysis-reforming process has shown great potential for H_2 production from biomass, with no operational problems and allowing for full conversion of pyrolysis vapours. Thus, a maximum H_2 yield of 117 g per kg of biomass was obtained at 600 °C, at the highest space time studied (30 g_{cat} min $g_{volatiles}^{-1}$) and for a S/B ratio of 4. This yield is higher than those obtained by other alternatives, such as direct steam gasification or bio-oil reforming. Moreover, the char produced in the pyrolysis step has been continuously removed from the conical spouted bed reactor in order to be upgraded following promising valorisation alternatives.

Received 19th January 2016
Accepted 1st March 2016

DOI: 10.1039/c6ra01657j

www.rsc.org/advances

Introduction

The promotion of H_2 as an energy carrier together with its increasing demand as a fuel and raw material has generated a growing interest for the development of renewable sources for its production, in order to modify the current situation in which around 96% of H_2 is produced from fossil fuels, such as natural gas, petroleum derivates or coal.[1]

The thermochemical conversion of biomass is an alternative for the full-scale production of H_2, and particularly gasification has been widely studied.[2] However, biomass gasification faces several challenges related to the quality of the syngas obtained and, especially, to its tar content, which causes serious operational problems due to the blockage by fouling of process equipment[3] and limits the applications of the syngas produced.[4]

Another alternative to produce H_2 from biomass that has gained growing attention in recent years is the indirect route by bio-oil reforming.[5] Bio-oil is the liquid product obtained in the biomass fast pyrolysis process, whose yield can reach 75 wt% operating under suitable conditions.[6,7] This strategy has certain clear advantages compared to the direct gasification, such as the remarkably lower process temperature, which gives way to lower energy requirements and material costs,[8] and the higher energy density of the bio-oil compared to biomass, leading to lower transport costs. However, the physical properties of the bio-oil pose a serious drawback for this indirect route. Thus, bio-oil is unstable and polymerizes under storage, causing an increase in viscosity and average molecular weight.[9] Furthermore, the incomplete vaporization of the bio-oil also involves a great challenge due to the formation of carbonaceous deposits, and therefore a decrease in the reforming conversion efficiency.[10] In order to alleviate the problems associated with bio-oil properties, most of the reforming studies in the literature have been carried out with model compounds and synthetic mixtures simulating bio-oil and tar[5,8] or with the bio-oil aqueous fraction.[11–13]

The H_2 production by biomass pyrolysis and in-line reforming of pyrolysis volatiles avoids the problems associated with bio-oil handling and vaporization. Furthermore, a fraction of the bio-oil is not discarded and all hydrocarbons of pyrolysis gases are reformed improving the potential process yield. Therefore, although it has been scarcely studied, this strategy is regarded as a feasible solution for H_2 production in small scale units.[14] The research group headed by Prof. Williams studied the pyrolysis and reforming of biomass and other residues in batch regime, with the unit consisting of two fixed bed reactors.[15–17] The process developed by the research group headed by Prof. Tomishige is also based on two fixed bed reactors for the pyrolysis and reforming steps and, although their experimental equipment is of a relatively reduced size, it operates with continuous biomass feed.[18,19] The process developed by Xiao *et al.*[20,21] is based on a fluidised bed reactor for the pyrolysis step and a fixed bed reactor for the catalytic steam reforming operating in continuous regime. The strategy proposed by Ma *et al.*[22] includes an intermediate char gasification step for the maximization of H_2 yield. Thus, the process

Department of Chemical Engineering, University of the Basque Country UPV/EHU, P.O. Box 644, E48080 Bilbao, Spain. E-mail: maider.amutio@ehu.es

consists of three sequential steps: pyrolysis in a fluidised bed reactor, char gasification in an entrained flow gasifier and reforming of volatiles in a fixed bed reactor.

In a previous paper,[23] a combination of a conical spouted bed reactor (CSBR) and a fixed bed reactor was used for the pyrolysis and in-line reforming of HDPE. In order to overcome the operational problems encountered when using a fixed bed in the reforming step, it has been replaced by a fluidised bed reactor.[24,25] Furthermore, the CSBR has shown an excellent performance in the pyrolysis of biomass,[6,26] which augurs well for a successful scale-up of the technology.[27]

This study pursues the development of an original continuous two-step process for the production of H_2 from biomass by coupling the pyrolysis in a CSBR with the steam reforming in a fluidised bed reactor. This direct strategy is an attractive and novel alternative to the indirect bio-oil reforming process, given that it avoids the operational problems associated with bio-oil handling. Moreover, the results were obtained in an experimental unit made up of two reactors connected in series operating in continuous regime and characterized by their high heat and mass transfer rates, and therefore, under similar conditions to those of industrial reactors.

Experimental

Materials

The biomass used in this study is forest pine wood waste (Pinus insignis), which has been crushed, ground and sieved to a particle size between 1 and 2 mm in order to ease the feeding operation. This sawdust has been dried at room temperature to moisture content below 10 wt% and the main properties are summarized in Table 1. The ultimate and proximate analyses have been determined in a LECO CHNS-932 elemental analyzer and in a TGA Q5000IR thermogravimetric analyzer, respectively. The higher heating value (HHV) has been measured in a Parr 1356 isoperibolic bomb calorimeter.

The catalyst used in the reforming step is a commercial one for methane reforming provided by Süd Chemie (G90LDP catalyst). The metallic phase is Ni supported on Al_2O_3, which is doped with Ca, with the content of NiO being 14%. The original catalyst has a shape of perforated rings (19 × 16 mm), but it was ground and sieved to 0.4–0.8 mm, which is the suitable particle size to attain a stable fluidisation regime.

Table 1 Pine wood sawdust characterization

Ultimate analysis (wt%)	
Carbon	49.33
Hydrogen	6.06
Nitrogen	0.04
Oxygen	44.57
Proximate analysis (wt%)	
Volatile matter	73.4
Fixed carbon	16.7
Ash	0.5
Moisture	9.4
HHV (MJ kg^{-1})	19.8

The physical properties of the catalyst have been determined by N_2 adsorption–desorption in a Micromeritics ASAP 2010. The adsorption–desorption isotherm of this catalyst, which has been reported elsewhere,[23,28] shows that it has low porosity with a BET surface area of 19 $m^2\ g^{-1}$ and an average pore diameter of 122 Å.

In order to determine the reduction conditions required prior to use, temperature programmed reduction (TPR) of the catalyst has been carried out in an AutoChem II 2920 Micromeritics. The TPR curve (provided in previous studies[23,28]) showed a main peak at 550 °C associated with NiO reduction, which interacts with α-Al_2O_3. Moreover, another peak is observed at 700 °C, which is probably related to $NiAl_2O_4$ according to the composition given by the provider.

Thus, the catalyst has been subjected to an *in situ* reduction process at 710 °C for 4 h under 10 vol% H_2 stream to ensure complete reduction of the metallic phase.

Equipment and reactors

The pyrolysis of biomass and in-line steam reforming of the volatiles produced has been studied in a bench scale plant whose scheme is shown in Fig. 1. The plant is provided with a CSBR for the pyrolysis step and a fluidised bed reactor for the reforming step.

The CSBR has been designed and tuned in previous studies dealing with hydrodynamics, pyrolysis and gasification of different wastes, such as biomass,[26,29,30] plastics[31,32] and tyres.[33,34]

The main dimensions of the pyrolysis reactor are as follows: height of the conical section, 73 mm; diameter of the cylindrical section, 60.3 mm; angle of the conical section, 30°; diameter of the bed bottom, 12.5 mm, and diameter of the gas inlet, 7.6

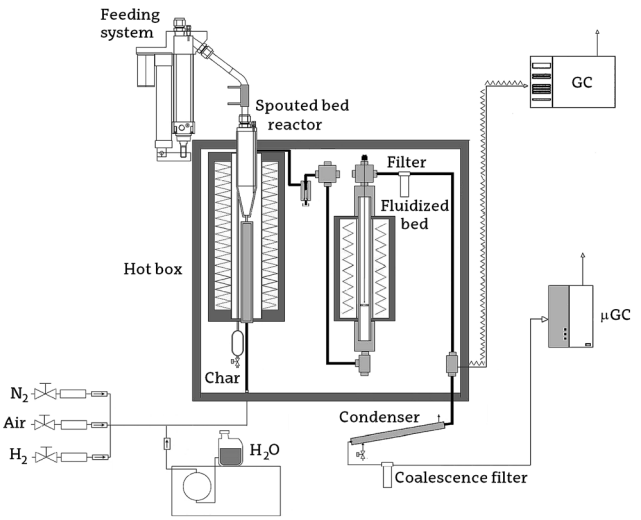

Fig. 1 Scheme of the laboratory scale pyrolysis-reforming plant.

mm. The reactor has a lateral outlet pipe placed above the bed surface for the removal of char particles from the bed (Fig. 1). Moreover, the reactor is provided with a gas preheater, which is filled with stainless steel pipes that increase the surface area for heat transfer. The reactor is located inside an oven of 1250 W, with this oven being controlled by two K-type thermocouples located inside the reactor, one in the bed annulus and the other one close to the wall.

The pyrolysis vapours formed in the pyrolysis process are reformed in a fluidised bed reactor. The diameter and length of this reactor are 38.1 and 440 mm, respectively. The heat required for the reforming step is provided by a 550 W radiant oven, which is controlled by a thermocouple placed in the catalyst bed.

Both the pyrolysis and the reforming reactors, together with the interconnection pipes, cyclone and filter are located inside a forced convection oven. This oven is kept at 270 °C in order to avoid the condensation of pyrolysis products and steam in the elements connecting the reaction system. The cyclone is placed downstream the pyrolysis reactor to retain the fine char particles entrained from the bed. Regarding the filter (5 μm sintered steel), its main purpose is to capture catalyst fines elutriated from the fluidised bed reactor.

The feeding system consists of a vessel equipped with a vertical shaft connected to a piston placed below the material bed. By raising the piston at the same time as the whole system is vibrated by an electric engine, the feeding system discharges the biomass through a pipe to the reactor. This pipe is cooled with tap water to avoid biomass partial degradation and blocking the system. Moreover, a very small nitrogen flow rate introduced into the vessel stops the steam entering the feeding vessel.

Experimental conditions

The operating conditions for the pyrolysis and reforming reactors were fine tuned in previous hydrodynamic studies carried out at the reaction temperatures (500 and 600 °C, respectively) in order to attain an adequate fluidisation behaviour in both steps. Therefore, not only the geometric factors of the reactors but also the size of sand particles in the pyrolysis reactor and those of sand and reforming catalyst in the reforming step have been optimized to achieve the desired fluidisation regime in each step.

Thus, the conical spouted bed reactor contains 50 g of silica sand with a particle size in the 0.3–0.35 mm range. The bed in the steam reforming step is made up of a mixture of reforming catalyst and inert sand, with the total bed mass being kept constant at 25 g in all the runs. The catalyst/sand mass ratios used were chosen according to the space time studied. The particle size of the catalyst was in the 0.4–0.8 mm range and that of the inert sand in the 0.3–0.35 mm range.

The temperature in the pyrolysis step was fixed at 500 °C in all the runs performed, because this temperature was determined as the optimum one in a previous study.[6] Table 2 summarizes the operating conditions used in the runs carried out for determining the influence of the parameters on the reforming step. The effect of temperature has been studied in the range from 550 to 700 °C, with steam/biomass ratio (S/B) and space time in these runs being 4 and 20 g_{cat} min $g_{volatiles}^{-1}$, respectively. The study of higher temperatures was discarded in order to avoid irreversible catalyst deactivation by sintering.

Table 2 Experimental conditions in the parametric study of the steam reforming step

Temperature (°C)	550, 600, 650 and 700 (space time 20, S/B 4)
S/B ratio[a]	2, 3, 4 and 5 (600 °C, space time 20)
S/C ratio	3.9, 5.8, 7.7 and 9.7 (600 °C, space time 20)
Space time (g_{cat} min g^{-1})[a]	2.1, 4.2, 8.3, 12.5, 16.7 and 25 (600 °C, S/B 4)
Space time (g_{cat} min g^{-1})[b]	2.5, 5, 10, 15, 20 and 30 (600 °C, S/B 4)

[a] By mass unit of the biomass fed into the pyrolysis reactor. [b] By molar unit of the pyrolysis derived volatiles fed into the reforming step, *i.e.* molar flow rate of carbon contained.

The influence of S/B ratio has been assessed by varying this parameter between 2 and 5, with the water flow rate being constant in all the runs (3 mL min^{-1}) in order to keep the hydrodynamic conditions in the reactors. Accordingly, the S/B ratio was adjusted by modifying the biomass feed rate in the range from 1.5 to 0.6 g min^{-1}. Moreover, the same space time (20 g_{cat} min $g_{volatiles}^{-1}$) was used in these runs, which was attained by modifying the mass of catalyst for each S/B ratio. Furthermore, in order to ease comparison of the results with those in the literature, the values have been determined for the molar steam/carbon ratio (S/C) of the stream fed into reforming step (biomass pyrolysis volatile fraction), Table 2. It should be noted that a char yield around 17 wt% is obtained in the pyrolysis step. Accordingly, the carbon contained in this char is not reformed in the second step and was not considered for the S/C ratio estimation.

Finally, the effect of space time in the reforming step was studied in the 2.5–30 g_{cat} min $g_{volatiles}^{-1}$ range by varying the amount of catalyst, with the biomass feed rate being kept at 0.75 g min^{-1}. In addition, the space times given by mass unit of the biomass fed into the pyrolysis reactor are also shown in Table 2.

All the runs have been performed in continuous mode for several minutes in order to ensure steady state in the process. Moreover, the runs have been repeated at least 3 times under the same conditions (with fresh catalyst) in order to guarantee reproducibility of the results.

Product analysis

The volatile stream leaving the reforming reactor has been analysed on-line by means of a GC Agilent 6890 provided with a HP-Pona column and a flame ionization detector (FID). The sample has been injected into the GC by means of a line thermostated at 280 °C, once the reforming reactor outlet stream has been diluted with an inert gas. The non-condensable gases have been analyzed on-line in a micro GC (Varian 4900) by taking the samples after the condenser and coalescence filter.

Reaction indexes

In order to quantify the process results, conversion and individual product yields have been considered. The reforming conversion has been defined similarly as the carbon conversion efficiency commonly used in the gasification processes, *i.e.*, the ratio between the moles of C recovered in the gaseous product and those fed into the reforming step.

$$X = \frac{C_{gas}}{C_{volatiles}} \times 100 \quad (1)$$

Note that the carbon contained in the biomass char is not considered for estimating conversion. Accordingly, full conversion of bio-oil compounds is attained when they are totally reformed to yield gaseous products. The bio-oil compounds yield has been determined by on-line GC analysis of the reformed product stream.

Similarly, the yield of C containing individual compounds has been based on the biomass pyrolysis volatiles stream

$$Y_i = \frac{F_i}{F_{volatiles}} \times 100 \quad (2)$$

where F_i and $F_{volatiles}$ are the molar flow rates of product i and pyrolysis volatiles, respectively, both given in C moles contained.

The hydrogen yield was determined as a percentage of the maximum allowed by stoichiometry, which accounts for the hydrogen coming from the pyrolysis products and the steam. The following stoichiometry was considered:

$$C_nH_mO_k + (2n - k)H_2O \rightarrow nCO_2 + (2n + m/2 - k)H_2 \quad (3)$$

$$Y_{H_2} = \frac{F_{H_2}}{F^0_{H_2}} \times 100 \quad (4)$$

where F_{H_2} and $F^0_{H_2}$ are the hydrogen molar flow rate obtained in the run and the maximum allowable by stoichiometry.

Results

Biomass pyrolysis (first step)

The pyrolysis step was carried out under steam environment, given that the steam required in the reforming step was introduced in the pyrolysis reactor, where it plays the role of a fluidising agent. A previous study revealed that steam has a negligible effect in the pyrolysis of this material, which is explained by the moderate temperature used in this process (500 °C). Moreover, it should be noted that, even operating with N_2 as fluidising agent, there is a significant steam concentration in the reaction environment because the water yield in the biomass pyrolysis process is above 25 wt%.[6] Thus, the results were similar to those previously reported by Amutio *et al.*[6] in the pyrolysis of the same biomass but using N_2 as fluidising agent. Kantarelis *et al.*[35] observed certain differences in the biomass pyrolysis product yields and composition when comparing steam and N_2 pyrolysis. However, the same authors stated based on a simulation study that the differences between steam and nitrogen pyrolysis are negligible in terms of heat transfer and product formation rate.[36]

The fast pyrolysis of pine wood sawdust in a CSBR gives way to a wide distribution of products, which can be grouped into three fractions: gases, bio-oil and char. The first two fractions are the volatile products, which are driven to the fluidised bed reactor to be reformed. However, the char formed is continuously removed from the pyrolysis reactor by means of a lateral outlet pipe to avoid its accumulation in the bed. This separation is achieved in the CSBR due to the different trajectories described by char particles in this system, which has previously been used in the pyrolysis of tyres and biomass, and has been described elsewhere.[26,33] Under the conditions studied, char yield is 17 wt% and its recovery is of great interest for the economy of the process, with its main applications being, amongst others, the production of adsorbent,[37,38] fertilizers,[39] catalyst support[40–42] and soil amender.[43]

The main product obtained in the pyrolysis step is the liquid product or bio-oil, whose yield is 75 wt% due to the excellent features of this reactor for biomass fast pyrolysis, especially, its high heat transfer rate, short residence time and rapid char removal from the reaction environment.[6] The main products of the bio-oil, which is a complex mixture of oxygenated compounds, are as follows: phenols (16.5 wt%), ketones (6.4%), saccharides (4.5%), furans (3.3%), acids (2.7%), alcohols (2.0%) and aldehydes (1.9%). Furthermore, a water yield of around 25 wt% is also obtained,[6] which acts also as a reforming agent in the second reforming step.

Regarding the gaseous fraction, its yield was 7.3 wt% and is made up of CO, CO_2 (similar yield for both, 3.3 wt%) and a low concentration of CH_4, C_2–C_4 hydrocarbons and H_2.[6]

The molecular formula corresponding to the stream of biomass pyrolysis volatiles entering the reforming reactor has been determined based on the compositions of the gas and bio-oil fractions: $CH_{1,93}O_{0,92}$.

Steam reforming (second step)

The effect of temperature, S/B ratio (or S/C ratio) and space time on the product yields and gas fraction composition have been analysed for the operating conditions summarized in Table 2. In order to ascertain the effect operating conditions have on the reaction indexes the following reactions have been considered: the steam reforming of oxygenates, eqn (3).

Water gas shift (WGS):

$$CO + H_2O \Leftrightarrow CO_2 + H_2 \quad (5)$$

Methane steam reforming:

$$CH_4 + H_2O \Leftrightarrow CO + 3H_2 \quad (6)$$

Cracking (secondary reaction):

$$C_nH_mO_k \rightarrow \text{oxygenates} + HCs + CH_4 + CO + CO_2 \quad (7)$$

Effect of temperature. The products obtained in the reforming step can be grouped into two fractions: the gaseous products and the non-converted liquids. The main gaseous products obtained in the reforming step are H_2, CO_2 and CO, and low concentrations of CH_4 and light hydrocarbons (C_2–C_4). The non-converted product fraction is mainly made up of bio-oil compounds leaving the pyrolysis step that have not been reformed, although changes would have undergone in their composition due to certain extent of thermal cracking in the reforming reactor.

The effect of temperature on biomass derived volatiles conversion is shown in Fig. 2. As observed, under the conditions studied at 550 °C conversion is almost 60%, whereas at 600 °C conversion is complete. Xiao *et al.*[20,21] studied the pyrolysis and in-line reforming of different biomasses on Ni catalysts in a fluidised-fixed bed system, and they also determined a minimum temperature of 600 °C to attain a high conversion degree of biomass tars.

Fig. 3 shows the effect of temperature on the individual gaseous product yields (graph a) and gas composition (graph b). It should be noted that H_2 yield is based on the maximum allowable by stoichiometry, but those of the other compounds are given by carbon mole unit fed into the reforming step. As observed in Fig. 3a, the effect of temperature on H_2 yield is negligible once full conversion has been reached (above 600 °C), with its yield being of around 93.5% between 600 and 700 °C. Consequently, 600 °C is considered the optimum temperature from a thermodynamic point of view, because it provides the highest equilibrium concentration for H_2 in the reforming of oxygenates.[8] In addition, operation at this relatively low temperature avoids the irreversible catalyst deactivation by Ni sintering.

Although most of the studies in the literature dealing with the steam reforming of bio-oil report lower H_2 yields based on the maximum allowable by stoichiometry than those in this study,[5] certain authors have reported values as high as 90% or even slightly higher.[12,13,44]

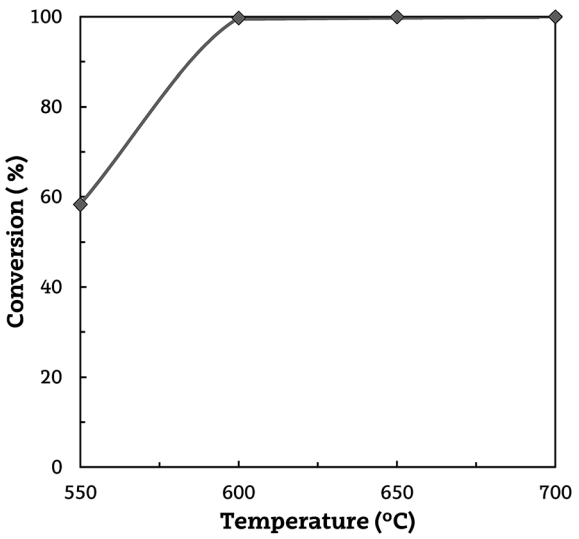

Fig. 2 Effect of reforming temperature on conversion. Reforming conditions: space time, 20 g_{cat} min $g_{volatiles}^{-1}$; S/B ratio, 4.

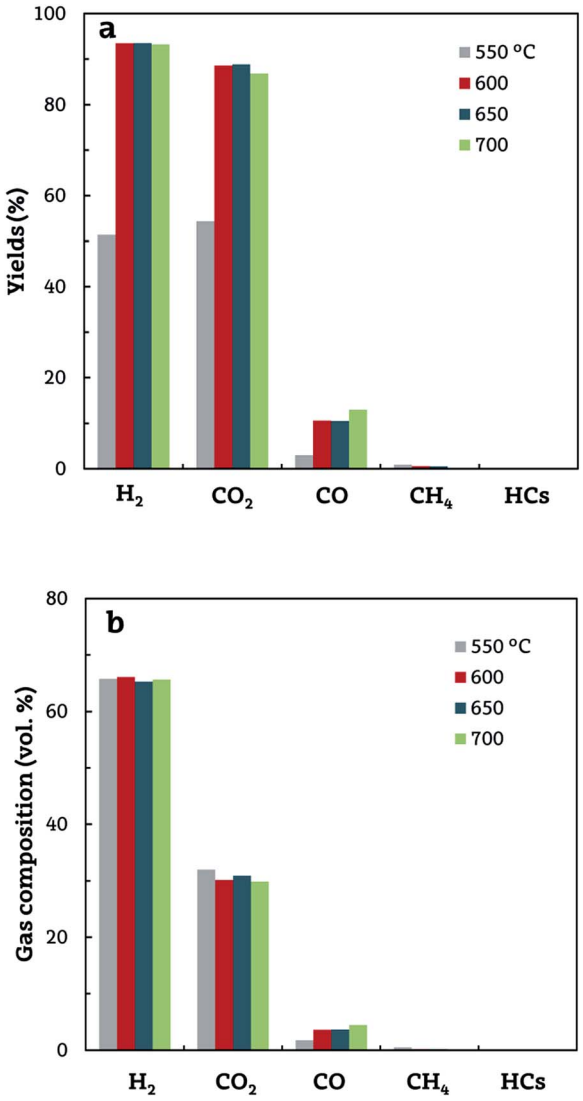

Fig. 3 Effect of reforming temperature on the yields of the gaseous products (a) and their concentrations (on a dry basis) (b). Reforming conditions: space time, 20 g_{cat} min $g_{volatiles}^{-1}$; S/B ratio, 4.

Regarding H_2 production, it increases from 64 g $kg_{biomass}^{-1}$ at 550 °C to around 110 g $kg_{biomass}^{-1}$ between 600 and 700 °C. Xiao *et al.*[20,21] reported a yield of around 100 g $kg_{biomass}^{-1}$ in the pyrolysis and in-line steam reforming of pine wood chips under optimum conditions in a fluidised-fixed bed system. Ma *et al.*[22] operated in a three-step process (biomass pyrolysis in a fluidised bed reactor, gasification in an entrained flow reactor and reforming in a fixed bed) and obtained a maximum H_2 yield of 76 g $kg_{biomass}^{-1}$ at the highest reforming temperature studied, 850 °C.

Furthermore, the H_2 yields reported in the biomass steam gasification process vary widely depending on the operating conditions, gasification technology, original biomass properties and, especially, on the type of catalyst used. Thus, when the gasification is performed with an inert material or a primary catalyst, such as dolomite, olivine or γ-alumina, the H_2 yields are between 30 and 50 g $kg_{biomass}^{-1}$.[45–48] The yields are higher,

70–80 g $kg_{biomass}^{-1}$, when the reforming activity is increased by improving the primary catalyst with the addition of Ni or Fe.[49,50]

A comparison of the H_2 production results with those in the indirect route, *i.e.* bio-oil reforming, is complex due to the differences between these two strategies. Thus, in the pyrolysis and in-line reforming process the carbon contained in the char fraction is not reformed, but the entire volatile fraction (including gases and the whole bio-oil) is treated. Nevertheless, the bio-oil reforming strategy has hardly been applied to the whole bio-oil, with the aqueous fraction being the feed in most of the cases. Furthermore, a significant fraction of the bio-oil is lost due to its incomplete vaporization.[10] Thus, problems related to phase separation of the raw bio-oil and the repolymerization of phenolic compounds, which have a great potential for H_2 production, hinder the feeding of the whole bio-oil into the reforming reactor.[51]

Furthermore, the fact that H_2 yields in the bio-oil reforming studies are referred to different basis, such as mass unit of organic compounds (without water), bio-oil aqueous fraction or whole bio-oil, also complicates comparison. Thus, the H_2 production obtained by Bimbela *et al.*[11] in the steam reforming of bio-oil aqueous phase on a Ni–Al catalyst was remarkably high, 138 g kg^{-1}, but their yield is given by mass unit of organic compounds in the feed. The value reported by Remiro *et al.*[52] in the reforming of raw bio-oil on a $Ni/La_2O_3–Al_2O_3$ catalyst is 117 g $kg_{bio\text{-}oil}^{-1}$. Salehi *et al.*[53] obtained a maximum H_2 production of 142 g $kg_{bio\text{-}oil}^{-1}$ in the reforming of raw bio-oil on a $Ni–Al_2O_3$ catalyst. The H_2 yield reported by Czernik and French[10] in the autho-thermal reforming of bio-oil aqueous fraction on a Pt commercial catalyst was slightly lower, between 85 and 110 g $kg_{bio\text{-}oil}^{-1}$, depending on the origin of the bio-oil tested. Accordingly, the indirect route has a lower H_2 production capacity per biomass mass unit compared to the direct pyrolysis-reforming strategy, even if high bio-oil yields are obtained (65–75 wt%) in the previous biomass pyrolysis process. Table 3 summarizes a comparison of the H_2 yields obtained in several biomass conversion processes.

It should be pointed out that both conversion and H_2 yield are strongly influenced by bio-oil composition, given that the reactivities of the compounds in the bio-oil are different. Most reforming studies in the literature focus on studying the effect of operating conditions, although certain authors conducted studies dealing with the reactivity of different model compounds in the bio-oil. Thus, Remón *et al.*[56] studied the catalytic reforming of acetic acid, phenol, furfural, guaiacol and levoglucosan on a Ni–Co/Al–Mg catalyst at 650 °C, and the H_2 yield obtained with the different model compounds followed this order: phenol > furfural > acetic acid > guaiacol > levoglucosan. The lower H_2 yields of guaiacol and levoglucosan were explained by the high amount of carbon converted into coke. 2-Methylfuran, furfural and guaiacol steam reforming were studied by Trane-Restrup and Jensen[57] and the highest temperature (780 °C) needed for complete conversion in the reforming of guaiacol was reported, whereas full conversion was achieved at 700 °C in the reforming of 2-methylfuran and furfural. Moreover, the highest carbon deposition was observed

Table 3 Comparison of H_2 and gas yields obtained in different biomass conversion processes

Reference	Strategy	Reactor	Feed	Temperature (°C)	Catalyst	H_2 yield (g kg^{-1})	Gas yield (m^3 kg^{-1})
This work	Pyrolysis/reforming	Spouted bed/ fluidised bed	Pine wood/pyrolysis volatiles	500/600	Ni commercial	110[a]	1.9[a]
20	Pyrolysis/reforming	Fluidised bed/ fixed bed	Pine wood/pyrolysis volatiles	650/650	Ni–coal char	100[a]	1.9[a]
21	Pyrolysis/reforming	Fixed bed/ fixed bed	Pine wood/pyrolysis volatiles	700/650	Ni–coal char	52[a]	1.12[a]
22	Pyrolysis/reforming	Fluidised bed/ fixed bed	Timber wood/pyrolysis volatiles	600/850	Ni–MgO commercial	76[a]	1.69[a]
54	Pyrolysis/reforming	Fixed bed/ fixed bed	Wood sawdust	500/800	$Ni–Ca–AlO_x$	31[a]	
11	Bio-oil reforming	Fixed bed	Bio-oil aqueous fraction	850	Ni–Al	138[b]	2.25[b]
53	Bio-oil reforming	Fixed bed	Raw bio-oil	950	$Ni–Ru–Al_2O_3$	142[c]	—
52	Bio-oil reforming	Fluidised bed	Raw bio-oil	700	$Ni–La_2O_3–Al_2O_3$	117[c]	1.85[c]
55	Bio-oil reforming	Fixed bed	Raw bio-oil	700	$Ni–Cu–Zn–Al_2O_3$	102[c]	1.6[c]
44	Bio-oil reforming	Fluidised bed	Raw bio-oil + 10% ethanol	850	Ni–K–Mg commercial	129[c]	2.1[c]
10	Oxidative bio-oil reforming	Fluidised bed	Bio-oil aqueous fraction	850	$Pt–Al_2O_3$ commercial	110[c]	1.9[c]
47	Steam gasification	Fluidised bed	Miscathus giganteus	880	Olivine	49[a]	1.2[a]
45	Steam gasification	Dual fluidised bed	Wood pellets	850	Olivine	42[a]	1.13[a]
48	Steam gasification	Spouted bed	Pine wood	900	Inert sand	32[a]	1[a]
46	Steam gasification	Updraft	Wood chips	700–900	—	36[a]	1[a]
50	Steam gasification	Fluidised bed	Miscathus giganteus	900	Ni–olivine	73[a]	1.6[a]
49	Steam gasification	Fluidised bed	Almond shell	830	Fe–olivine	65[a]	1.4[a]

[a] Yields per kg of biomass. [b] Yields per kg of organic bio-oil. [c] Yields per kg of bio-oil.

for guaiacol followed by furfural and 2-methylfuran. Wang *et al.*[58] investigated the steam reforming of phenol, acetic acid and hydroxyacetone at 700 °C on a Ni/nano-Al_2O_3 catalyst and the conversion and H_2 yield decrease as follows: hydroxyacetone > acetic acid > phenol. Some model compounds of bio-oil were also studied by Hu and Lu[59] at temperatures below 500 °C for the steam reforming of acetic acid, ethylene glycol and acetone, while higher temperatures were needed for the reforming of ethyl acetate and *m*-xylene.

Nevertheless, the reactivity of these compounds is different when they are reformed alone or in a mixture of different organic compounds. These interactions were studied by Remón *et al.*[56] and a different reactivity was reported for the acetic acid depending on the medium. Thus, 100% conversion was achieved for the reforming of an aqueous solution of acetic acid, whereas 87% of the acetic acid was converted in the reforming of the aqueous fraction of the bio-oil. Wu *et al.*[60] studied the difference between two simulated aqueous fractions of bio-oil, a light fraction (methanol, ethanol, acetic acid and acetone mixture) and a heavy fraction (furfural, phenol, catechol and *m*-cresol mixture), and they report that higher temperatures are needed for reforming the heavy fraction, with coke deposition being more significant. Consequently, the difficulty is evident in studying the reactivity of the compounds of biomass pyrolysis volatiles, due to the high amount of species contained and the interactions between them.

Carbon monoxide and dioxide yields are enhanced by increasing reforming temperature from 550 to 600 °C (Fig. 3a). However, above 600 °C, an increase in CO is observed at the expense of decreasing CO_2, with this trend being related to the exothermic nature of the WGS reaction (eqn (5)), which is hindered by temperature.

The effect of temperature on the gaseous fraction composition is not so remarkable (Fig. 3b). In fact, H_2 concentration takes values of around 66 vol% in the range studied. A slight effect on CO_2 and, especially, on CO concentration is observed, with their evolution being explained by the effect of temperature on the WGS reaction equilibrium. The slight differences between the gas composition obtained at 550 and 600 °C, but great differences in conversion, are explained by the fact that almost all the gases are produced by reforming. Thus, the formation of gases by secondary reactions involving pyrolysis products, *i.e.*, cracking, decarboxylation, decarbonilation and so on, are of minor significance.

Effect of space time. As observed in Fig. 4, a value of 20 g_{cat} min $g_{volatiles}^{-1}$ is required to attain pyrolysis volatiles full conversion. However, operating with 15 g_{cat} min $g_{volatiles}^{-1}$ the process performance is also suitable, obtaining a conversion of 98.5%. Consequently, specific gas production increases with space time, reaching a value of 1.95 N m^3 $kg_{biomass}^{-1}$ for the highest space time studied. This production is considerably higher than those usually reported for the steam gasification of biomass, even though partial conversion of char occurs in gasification. Thus, the specific gas production usually ranges between 0.9 and 1.2 N m^3 $kg_{biomass}^{-1}$ operating under suitable conditions,[45–48] reaching values of up to 1.7 N m^3 $kg_{biomass}^{-1}$ when using *in situ* catalysts.[50] Nevertheless, it should be noted

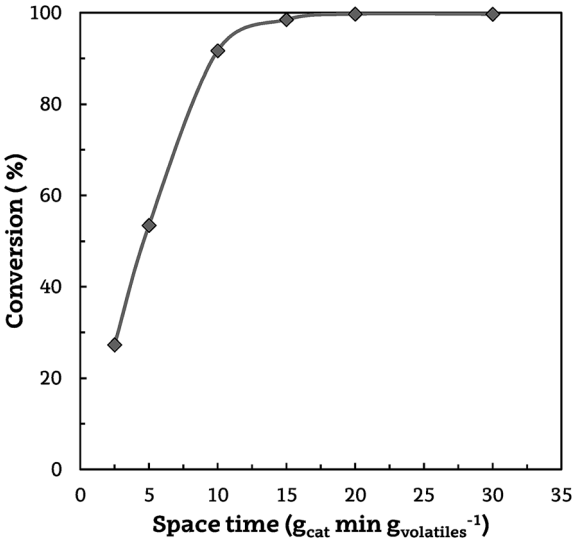

Fig. 4 Effect of reforming space time on conversion. Reforming conditions: 600 °C; S/B ratio, 4.

that the main advantage of the pyrolysis-reforming strategy compared to gasification is the capability for producing a H_2 rich gas free of tars (the main challenge in gasification) by taking advantage of highly active reforming catalysts. Therefore, the pyrolysis-reforming strategy should be conducted with relatively high space times in order to ensure a gas product completely free of tars, which would also ease its subsequent applications.

An increase in space time enhances both steam reforming (eqn (3)) and WGS (eqn (5)) reactions, and therefore the formation of H_2, CO_2 and CO is favoured, as shown in Fig. 5a. It should be noted that, for the highest space time studied (30 g_{cat} min $g_{volatiles}^{-1}$), CO yield decreases due to the displacement of the WGS reaction. This fact, together with the intensification of CH_4 and other hydrocarbon reforming, gives way to an increase in H_2 yield, reaching a value of 95.8% of the maximum allowable by stoichiometry. A qualitatively similar effect of space time on product yields has been observed by several authors in the steam reforming of bio-oil.[52,61,62]

Furthermore, hydrogen mass balance (considering the hydrogen content in the volatiles, the water fed into the reaction medium and the H_2 produced) allows verifying that the water reacted increases when space time is increased. This value is negative for 2.5 g_{cat} min $g_{volatiles}^{-1}$ because the inner biomass moisture is not consumed, whereas for 30 g_{cat} min $g_{volatiles}^{-1}$ the water reacted accounts for 522 g $kg_{biomass}^{-1}$ and the H_2 produced for 117 g $kg_{biomass}^{-1}$.

The influence of space time on gas fraction composition is shown in Fig. 5b. As observed, the main effect of increasing space time is an increase in H_2 and CO_2 concentration and a decrease in that of CO. In addition, a remarkable improvement of CH_4 conversion is also observed.

Effect of steam/biomass ratio. Fig. 6 shows the effect of S/B ratio on process conversion. As observed, the effect is almost negligible due to the high conversion values obtained for all the S/B ratios studied. This result can be attributed to the

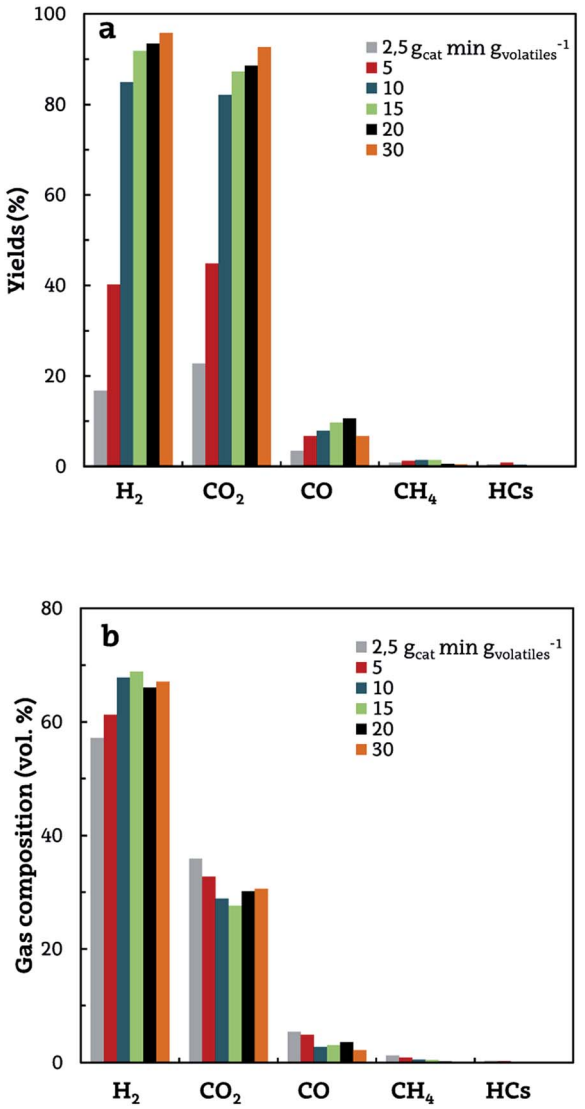

Fig. 5 Effect of reforming space time on the yields of gaseous products (a) and their concentrations (on a dry basis) (b). Reforming conditions: 600 °C; S/B ratio, 4.

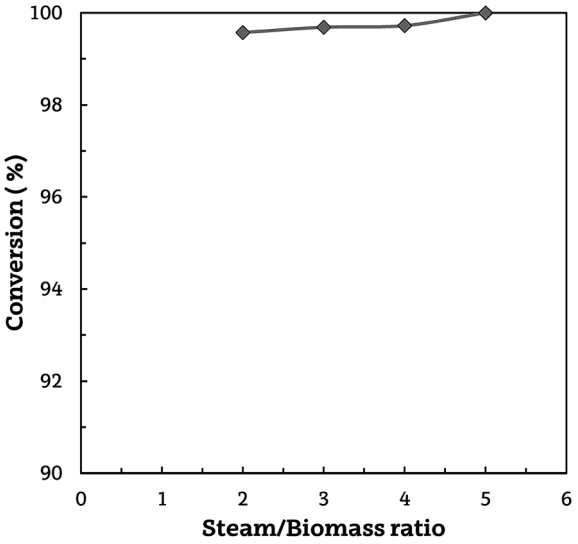

Fig. 6 Effect of S/B ratio on conversion. Reforming conditions: 600 °C; space time, 20 g_{cat} min $g_{volatiles}^{-1}$.

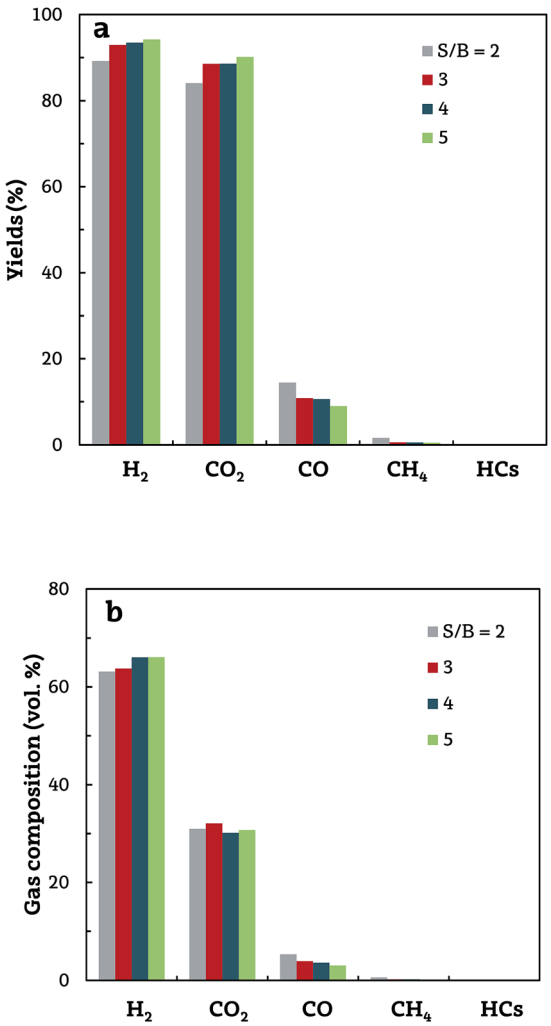

Fig. 7 Effect of S/B ratio on the yields of the gaseous products (a) and their concentrations (on a dry basis) (b). Reforming conditions: 600 °C; space time, 20 g_{cat} min $g_{volatiles}^{-1}$.

relatively high space time studied, which ensures high conversion values.

Furthermore, as observed in Fig. 7a, the effect of S/B ratio on the yields of the individual compounds is more noticeable. Thus, an increase in S/B ratio causes a steady increase in H_2 and CO_2 yields and a reduction in those of CO and CH_4. An increase in the steam partial pressure in the reaction environment enhances steam reforming reaction kinetics (eqn (3) and (6)), as well as the displacement of the WGS reaction equilibrium (eqn (5)). Thus, H_2 yield increases from 89.2% to 94.2% when S/B ratio is raised from 2 to 5, although a similar conversion is attained in both experiments. In the same line, the yield of CO_2 increases from 84.0 to 90.1%, whereas the opposite trend is observed for CO, *i.e.*, a decrease from 14.4 to 8.9%. The same effect of S/B ratio on product yields has been reported by other

authors in the reforming of bio-oil and pyrolysis vapours[20,52,61] and in the biomass steam gasification.[48,63]

Although process conversion efficiency improves for high S/B ratios and reduces coke formation,[5] this parameter should be carefully optimized bearing in mind energy efficiency,[20] *i.e.*, high S/B ratios require high amounts of steam to be produced and unreacted steam to be condensed at the outlet of the reformer. The optimum S/B ratios determined for biomass steam gasification are in the 0.6–0.85 range,[64] but those for the pyrolysis-reforming strategy should be higher due to the higher steam consumption.

As observed in Fig. 7b, the effect of S/B ratio on the concentration of gaseous products is qualitatively similar to the effect on product yields. H_2 concentration increases with S/B ratio to a value of 66.1 vol% for an S/B value of 5. However, CO content in the gas decreases from 5.3 to 3.0 vol% in the S/B ratio range studied. The CO_2 concentration does not follow a clear trend, with its concentration being between 30 and 32 vol%. The content of CH_4 and other gaseous hydrocarbons is very low due to the relatively high space time used.

Conclusions

The pyrolysis of biomass in a CSBR and in-line reforming in a fluidised bed reactor has proven to be a feasible alternative for the production of H_2. The separation of pyrolysis and reforming steps has several practical advantages, both from an operational point of view and from the catalytic reforming performance. Moreover, steam atmosphere in the pyrolysis has a limited effect on product distribution, with the results being similar to those previously obtained using N_2 as fluidising agent.

The Ni commercial catalyst is highly active for the reforming of biomass pyrolysis volatiles. A minimum temperature of 600 °C and a space time of 20 g_{cat} min $g_{volatiles}^{-1}$ are required to attain complete conversion with an S/B ratio of 4. Once this temperature has been reached, a further increase to 700 °C showed a limited effect on product yield and composition, with H_2 production being 110 g $kg_{biomass}^{-1}$ in this temperature range.

An increase in space time enhances both the reforming and the WGS reaction, leading to an increase in the yields of H_2 and CO_2. Thus, at the highest space time studied, a H_2 yield of 95.8% of the maximum allowable by stoichiometry was obtained. Similarly, the main effect of increasing the S/B ratio is the shifting of the reforming and WGS reactions, thereby improving H_2 yield. However, an increase in this ratio involves higher heating requirements in the process.

Acknowledgements

This work was carried out with financial support from the Ministry of Economy and Competitiveness of the Spanish Government (CTQ2013-45105 R and CTQ2014-59574-JIN), the EDRF funds, the Basque Government (IT748-13) and the University of the Basque Country (UFI 11/39).

References

1 H. Balat and E. Kirtay, Hydrogen from biomass - Present scenario and future prospects, *Int. J. Hydrogen Energy*, 2010, **35**, 7416–7426.
2 A. A. Ahmad, N. A. Zawawi, F. H. Kasim, A. Inayat and A. Khasri, Assessing the gasification performance of biomass: A review on biomass gasification process conditions, optimization and economic evaluation, *Renewable Sustainable Energy Rev.*, 2016, **53**, 1333–1347.
3 S. Anis and Z. A. Zainal, Tar reduction in biomass producer gas via mechanical, catalytic and thermal methods: A review, *Renewable Sustainable Energy Rev.*, 2011, **15**, 2355–2377.
4 P. J. Woolcock and R. C. Brown, A review of cleaning technologies for biomass-derived syngas, *Biomass Bioenergy*, 2013, **52**, 54–84.
5 R. Trane, S. Dahl, M. S. Skjoth-Rasmussen and A. D. Jensen, Catalytic steam reforming of bio-oil, *Int. J. Hydrogen Energy*, 2012, **37**, 6447–6472.
6 M. Amutio, G. Lopez, M. Artetxe, G. Elordi, M. Olazar and J. Bilbao, Influence of temperature on biomass pyrolysis in a conical spouted bed reactor, *Resour., Conserv. Recycl.*, 2012, **59**, 23–31.
7 Z. Ma, L. Wei, W. Zhou, L. Jia, B. Hou, D. Li and Y. Zhao, Overview of catalyst application in petroleum refinery for biomass catalytic pyrolysis and bio-oil upgrading, *RSC Adv.*, 2015, **5**, 88287–88297.
8 A. A. Lemonidou, P. Kechagiopoulos, E. Heracleous and S. Voutetakis, Steam Reforming of Bio-oils to Hydrogen, *The Role of Catalyst for the Sustainaible Production of Bio-Fuels and Bio-Chemicals*, 2013, pp. 467–493.
9 A. Demirbas, Competitive liquid biofuels from biomass, *Appl. Energy*, 2011, **88**, 17–28.
10 S. Czernik and R. French, Distributed production of hydrogen by auto-thermal reforming of fast pyrolysis bio-oil, *Int. J. Hydrogen Energy*, 2014, **39**, 744–750.
11 F. Bimbela, M. Oliva, J. Ruiz, L. García and J. Arauzo, Hydrogen production via catalytic steam reforming of the aqueous fraction of bio-oil using nickel-based coprecipitated catalysts, *Int. J. Hydrogen Energy*, 2013, **38**, 14476–14487.
12 B. Valle, A. Remiro, A. T. Aguayo, J. Bilbao and A. G. Gayubo, Catalysts of Ni/Al_2O_3 and Ni/La_2O_3-Al_2O_3 for hydrogen production by steam reforming of bio-oil aqueous fraction with pyrolytic lignin retention, *Int. J. Hydrogen Energy*, 2013, **38**, 1307–1318.
13 P. N. Kechagiopoulos, S. S. Voutetakis, A. A. Lemonidou and I. A. Vasalos, Hydrogen production via reforming of the aqueous phase of bio-oil over Ni/olivine catalysts in a spouted bed reactor, *Ind. Eng. Chem. Res.*, 2009, **48**, 1400–1408.
14 T. Namioka, A. Saito, Y. Inoue, Y. Park, T. j. Min, S. a. Roh and K. Yoshikawa, Hydrogen-rich gas production from waste plastics by pyrolysis and low-temperature steam reforming over a ruthenium catalyst, *Appl. Energy*, 2011, **88**, 2019–2026.

15 J. Alvarez, S. Kumagai, C. Wu, T. Yoshioka, J. Bilbao and M. Olazar, Hydrogen production from biomass and plastic mixtures by pyrolysis-gasification, *Int. J. Hydrogen Energy*, 2014, **39**, 10883–10891.
16 M. A. Nahil, X. Wang, C. Wu, H. Yang, H. Chen and P. T. Williams, Novel bi-functional Ni-Mg-Al-CaO catalyst for catalytic gasification of biomass for hydrogen production with in situ CO_2 adsorption, *RSC Adv.*, 2013, **3**, 5583–5590.
17 A. K. Olaleye, K. J. Adedayo, C. Wu, M. A. Nahil, M. Wang and P. T. Williams, Experimental study, dynamic modelling, validation and analysis of hydrogen production from biomass pyrolysis/gasification of biomass in a two-stage fixed bed reaction system, *Fuel*, 2014, **137**, 364–374.
18 M. Koike, C. Ishikawa, D. Li, L. Wang, Y. Nakagawa and K. Tomishige, Catalytic performance of manganese-promoted nickel catalysts for the steam reforming of tar from biomass pyrolysis to synthesis gas, *Fuel*, 2013, **103**, 122–129.
19 L. Wang, D. Li, M. Koike, S. Koso, Y. Nakagawa, Y. Xu and K. Tomishige, Catalytic performance and characterization of Ni-Fe catalysts for the steam reforming of tar from biomass pyrolysis to synthesis gas, *Appl. Catal., A*, 2011, **392**, 248–255.
20 X. Xiao, X. Meng, D. D. Le and T. Takarada, Two-stage steam gasification of waste biomass in fluidized bed at low temperature: Parametric investigations and performance optimization, *Bioresour. Technol.*, 2011, **102**, 1975–1981.
21 X. Xiao, J. Cao, X. Meng, D. D. Le, L. Li, Y. Ogawa, K. Sato and T. Takarada, Synthesis gas production from catalytic gasification of waste biomass using nickel-loaded brown coal char, *Fuel*, 2013, **103**, 135–140.
22 Z. Ma, S. Zhang, D. Xie and Y. Yan, A novel integrated process for hydrogen production from biomass, *Int. J. Hydrogen Energy*, 2014, **39**, 1274–1279.
23 A. Erkiaga, G. Lopez, I. Barbarias, M. Artetxe, M. Amutio, J. Bilbao and M. Olazar, HDPE pyrolysis-steam reforming in a tandem spouted bed-fixed bed reactor for H_2 production, *J. Anal. Appl. Pyrolysis*, 2015, **116**, 34–41.
24 A. Remiro, B. Valle, B. Aramburu, A. T. Aguayo, J. Bilbao and A. G. Gayubo, Steam reforming of the bio-oil aqueous fraction in a fluidized bed reactor with in situ CO_2 capture, *Ind. Eng. Chem. Res.*, 2013, **52**, 17087–17098.
25 P. Lan, Q. Xu, M. Zhou, L. Lan, S. Zhang and Y. Yan, Catalytic steam reforming of fast pyrolysis bio-oil in fixed bed and fluidized bed reactors, *Chem. Eng. Technol.*, 2010, **33**, 2021–2028.
26 M. Amutio, G. Lopez, R. Aguado, J. Bilbao and M. Olazar, Biomass Oxidative Flash Pyrolysis: Autothermal Operation, Yields and Product Properties, *Energy Fuels*, 2012, **26**, 1353–1362.
27 J. Makibar, A. R. Fernandez-Akarregi, M. Amutio, G. Lopez and M. Olazar, Performance of a conical spouted bed pilot plant for bio-oil production by poplar flash pyrolysis, *Fuel Process. Technol.*, 2015, **137**, 283–289.
28 G. Lopez, A. Erkiaga, M. Artetxe, M. Amutio, J. Bilbao and M. Olazar, Hydrogen Production by High Density Polyethylene Steam Gasification and In-Line Volatile Reforming, *Ind. Eng. Chem. Res.*, 2015, **54**, 9536–9544.
29 J. Alvarez, M. Amutio, G. Lopez, I. Barbarias, J. Bilbao and M. Olazar, Sewage sludge valorization by flash pyrolysis in a conical spouted bed reactor, *Chem. Eng. J.*, 2015, **273**, 173–183.
30 A. Erkiaga, G. Lopez, M. Amutio, J. Bilbao and M. Olazar, Steam gasification of biomass in a conical spouted bed reactor with olivine and γ-alumina as primary catalysts, *Fuel Process. Technol.*, 2013, **116**, 292–299.
31 A. Erkiaga, G. Lopez, M. Amutio, J. Bilbao and M. Olazar, Syngas from steam gasification of polyethylene in a conical spouted bed reactor, *Fuel*, 2013, **109**, 461–469.
32 M. Artetxe, G. Lopez, G. Elordi, M. Amutio, J. Bilbao and M. Olazar, Production of Light Olefins from Polyethylene in a Two-Step Process: Pyrolysis in a Conical Spouted Bed and Downstream High-Temperature Thermal Cracking, *Ind. Eng. Chem. Res.*, 2012, **51**, 13915–13923.
33 G. Lopez, M. Olazar, M. Amutio, R. Aguado and J. Bilbao, Influence of Tire Formulation on the Products of Continuous Pyrolysis in a Conical Spouted Bed Reactor, *Energy Fuels*, 2009, **23**, 5423–5431.
34 G. Lopez, M. Olazar, R. Aguado, G. Elordi, M. Amutio, M. Artetxe and J. Bilbao, Vacuum Pyrolysis of Waste Tires by Continuously Feeding into a Conical Spouted Bed Reactor, *Ind. Eng. Chem. Res.*, 2010, **49**, 8990–8997.
35 E. Kantarelis, W. Yang and W. Blasiak, Production of liquid feedstock from biomass via steam pyrolysis in a fluidized bed reactor, *Energy Fuels*, 2013, **27**, 4748–4759.
36 P. Mellin, E. Kantarelis, C. Zhou and W. Yang, Simulation of bed dynamics and primary products from fast pyrolysis of biomass: Steam compared to nitrogen as a fluidizing agent, *Ind. Eng. Chem. Res.*, 2014, **53**, 12129–12142.
37 J. Alvarez, G. Lopez, M. Amutio, J. Bilbao and M. Olazar, Upgrading the rice husk char obtained by flash pyrolysis for the production of amorphous silica and high quality activated carbon, *Bioresour. Technol.*, 2014, **170**, 132–137.
38 S. Wang, B. Gao, Y. Li, Y. Wan and A. E. Creamer, Sorption of arsenate onto magnetic iron-manganese (Fe-Mn) biochar composites, *RSC Adv.*, 2015, **5**, 67971–67978.
39 M. Uchimiya, S. Hiradate and M. J. Antal, Dissolved Phosphorus Speciation of Flash Carbonization, Slow Pyrolysis, and Fast Pyrolysis Biochars, *ACS Sustainable Chem. Eng.*, 2015, **3**, 1642–1649.
40 C. M. Dominguez, P. Ocon, A. Quintanilla, J. A. Casas and J. J. Rodriguez, Highly efficient application of activated carbon as catalyst for wet peroxide oxidation, *Appl. Catal., B*, 2013, **140–141**, 663–670.
41 S. Ren, H. Lei, L. Wang, Q. Bu, S. Chen and J. Wu, Hydrocarbon and hydrogen-rich syngas production by biomass catalytic pyrolysis and bio-oil upgrading over biochar catalysts, *RSC Adv.*, 2014, **4**, 10731–10737.
42 Y. Shen, C. Areeprasert, B. Prabowo, F. Takahashi and K. Yoshikawa, Metal nickel nanoparticles in situ generated in rice husk char for catalytic reformation of tar and syngas from biomass pyrolytic gasification, *RSC Adv.*, 2014, **4**, 40651–40664.

43 C. R. Smith, E. M. Buzan and J. W. Lee, Potential impact of biochar water-extractable substances on environmental sustainability, *ACS Sustainable Chem. Eng.*, 2013, **1**, 118–126.
44 S. Czernik, R. Evans and R. French, Hydrogen from biomass-production by steam reforming of biomass pyrolysis oil, *Catal. Today*, 2007, **129**, 265–268.
45 S. Koppatz, C. Pfeifer and H. Hofbauer, Comparison of the performance behaviour of silica sand and olivine in a dual fluidised bed reactor system for steam gasification of biomass at pilot plant scale, *Chem. Eng. J.*, 2011, **175**, 468–483.
46 K. Umeki, K. Yamamoto, T. Namioka and K. Yoshikawa, High temperature steam-only gasification of woody biomass, *Appl. Energy*, 2010, **87**, 791–798.
47 R. Michel, S. Rapagna, P. Burg, d. C. Mazziotti, C. Courson, T. Zimny and R. Gruber, Steam gasification of Miscanthus X Giganteus with olivine as catalyst production of syngas and analysis of tars (IR, NMR and GC/MS), *Biomass Bioenergy*, 2011, **35**, 2650–2658.
48 A. Erkiaga, G. Lopez, M. Amutio, J. Bilbao and M. Olazar, Influence of operating conditions on the steam gasification of biomass in a conical spouted bed reactor, *Chem. Eng. J.*, 2014, **237**, 259–267.
49 S. Rapagna, M. Virginie, K. Gallucci, C. Courson, M. Di Marcello, A. Kiennemann and P. U. Foscolo, Fe/olivine catalyst for biomass steam gasification: Preparation, characterization and testing at real process conditions, *Catal. Today*, 2011, **176**, 163–168.
50 R. Michel, S. Rapagna, M. Di Marcello, P. Burg, M. Matt, C. Courson and R. Gruber, Catalytic steam gasification of Miscanthus X giganteus in fluidised bed reactor on olivine based catalysts, *Fuel Process. Technol.*, 2011, **92**, 1169–1177.
51 C. Rioche, S. Kulkarni, F. C. Meunier, J. P. Breen and R. Burch, Steam reforming of model compounds and fast pyrolysis bio-oil on supported noble metal catalysts, *Appl. Catal., B*, 2005, **61**, 130–139.
52 A. Remiro, B. Valle, A. T. Aguayo, J. Bilbao and A. G. Gayubo, Steam reforming of raw bio-oil in a fluidized bed reactor with prior separation of pyrolytic lignin, *Energy Fuels*, 2013, **27**, 7549–7559.
53 E. Salehi, F. S. Azad, T. Harding and J. Abedi, Production of hydrogen by steam reforming of bio-oil over Ni/Al_2O_3 catalysts: Effect of addition of promoter and preparation procedure, *Fuel Process. Technol.*, 2011, **92**, 2203–2210.
54 F. Chen, C. Wu, L. Dong, A. Vassallo, P. T. Williams and J. Huang, Characteristics and catalytic properties of $Ni/CaAlO_x$ catalyst for hydrogen-enriched syngas production from pyrolysis-steam reforming of biomass sawdust, *Appl. Catal., B*, 2016, **183**, 168–175.
55 T. Kan, J. Xiong, X. Li, T. Ye, L. Yuan, Y. Torimoto, M. Yamamoto and Q. Li, High efficient production of hydrogen from crude bio-oil via an integrative process between gasification and current-enhanced catalytic steam reforming, *Int. J. Hydrogen Energy*, 2010, **35**, 518–532.
56 J. Remón, F. Broust, G. Volle, L. García and J. Arauzo, Hydrogen production from pine and poplar bio-oils by catalytic steam reforming. Influence of the bio-oil composition on the process, *Int. J. Hydrogen Energy*, 2015, **40**, 5593–5608.
57 R. Trane-Restrup and A. D. Jensen, Steam reforming of cyclic model compounds of bio-oil over Ni-based catalysts: Product distribution and carbon formation, *Appl. Catal., B*, 2015, **165**, 117–127.
58 S. Wang, Q. Cai, F. Zhang, X. Li, L. Zhang and Z. Luo, Hydrogen production via catalytic reforming of the bio-oil model compounds: Acetic acid, phenol and hydroxyacetone, *Int. J. Hydrogen Energy*, 2014, **39**, 18675–18687.
59 X. Hu and G. Lu, Investigation of the steam reforming of a series of model compounds derived from bio-oil for hydrogen production, *Appl. Catal., B*, 2009, **88**, 376–385.
60 C. Wu, M. Sui and Y. Yan, A comparison of steam reforming of two model bio-oil fractions, *Chem. Eng. Technol.*, 2008, **31**, 1748–1753.
61 P. Fu, W. Yi, Z. Li, X. Bai, A. Zhang, Y. Li and Z. Li, Investigation on hydrogen production by catalytic steam reforming of maize stalk fast pyrolysis bio-oil, *Int. J. Hydrogen Energy*, 2014, **39**, 13962–13971.
62 F. Seyedeyn-Azad, E. Salehi, J. Abedi and T. Harding, Biomass to hydrogen via catalytic steam reforming of bio-oil over Ni-supported alumina catalysts, *Fuel Process. Technol.*, 2011, **92**, 563–569.
63 K. Goransson, U. Soderlind and W. Zhang, Experimental test on a novel dual fluidised bed biomass gasifier for synthetic fuel production, *Fuel*, 2011, **90**, 1340–1349.
64 P. Kaushal and R. Tyagi, Steam assisted biomass gasification-an overview, *Can. J. Chem. Eng.*, 2012, **90**, 1043–1058.